07,01

Study of the structural features of microcrystalline aluminum after tests for long-term strength

© S.S. Manohin[1], V.I. Betekhtin[2], A.G. Kadomtsev[2,¶], M.V. Narykova[2], O.V. Amosova[2], Yu.R. Kolobov[1], D.V. Lazarev[1]

[1] Institute of Problems of Chemical Physics, Russian Academy of Sciences, Chernogolovka, Moscow oblast, Russia
[2] Ioffe Institute, St. Petersburg, Russia

¶ E-mail: andrej.kadomtsev@mail.ioffe.ru

Received September 30, 2022
Revised: September 30, 2022
Accepted October 1, 2022

The effect of creep on changes in the structure of samples of recrystallized microcrystalline aluminum in the fracture region and at some distance from it is studied. Transmission and scanning electron microscopy have been used to study the features of the formation of a globular ultrafine-grained structure in the region of destruction with a minimum manifestation of crystallographic texture, as well as the presence of micro- and nanoporosity.

Keywords: aluminum, creep, microstructure, electron microscopy, nanopores.

DOI: 10.21883/PSS.2023.01.54986.492

1. Introduction

One of the fundamental problems of strength physics is the problem of assessing the operational life (durability) of structural metals and alloys and the development of methods to improve it. It is known, that under conditions of simultaneous exposure to temperature and load in metallic materials, the formation of pores and cracks occurs at the early stages of plastic deformation. As a result, plastic loosening (decrease in density) accumulates in the materials during the entire stay under load, mainly due to the formation of damage in the form of multi-scale pores and cracks [1–3]. For the submicrograin metallics (SMG) obtained by the Intensive Plastic Deformation (IPD) methods, the analysis of the evolution of damage under prolonged load should also take into account the presence and „of the initial" (before loading) nanoscale porosity [4]. The formation of such nanoporosity due to IPD is described in a number of papers [5–12].

Identification of the parameters of the defective structure of the material contributing to the transition to macro-destruction, as well as the kinetic patterns of the origin and growth of cracks under prolonged loads is important both for understanding the physical nature of the destruction of metals and alloys, and for developing methods for evaluating and improving their performance (durability) [13–15].

At the moment, in the domestic and foreign literature, issues related to the contribution of forming defects (nanopores and microcracks) are considered quite relevant, both during the processes of intensive (severe) plastic deformation and during subsequent tests for long-term strength of microcrystalline metals and alloys.

In view of the above, the purpose of this work was to study by modern analytical methods of transmission and scanning electron microscopy the effect of creep deformation on structural changes of recrystallized microcrystalline aluminum, as well as to identify the features of the formation and growth of nanopores and cracks.

2. Material and research techniques

The study was conducted on the example of aluminum grade AD1. The elemental composition of the alloy under study is given in the table.

Previously, modes of mechanical and thermal treatment of alloys of technically pure titanium and aluminum of various grades were developed using longitudinal and transverse screw rolling, allowing to obtain rods of titanium and aluminum SMG with diameters of 4–10 mm [16]. In this work, aluminum alloy rods AD1 ∅8 mm were used in the SMG state, which were subjected to recrystallization annealing at a temperature of 250°C during 1 hour.

After this treatment, the alloy is characterized by a homogeneous grain-subgrain structure with an arithmetic mean size of structural elements of the order of 1.5 μm, further designated as microcrystalline aluminum.

The object of research were samples after creep tests (long-term strength) at a voltage of 75 MPa, for 8700 s at a temperature of 200°C. Samples for transmission electron microscopy were prepared by the focused ion beam method from the sample destruction area after creep tests.

The microstructure of the samples was studied by the transmission diffraction electron microscopy (TEM) on a FEI Tecnai Osiris microscope at an accelerating stress of 20 kV (including in the mode of scanning transmission

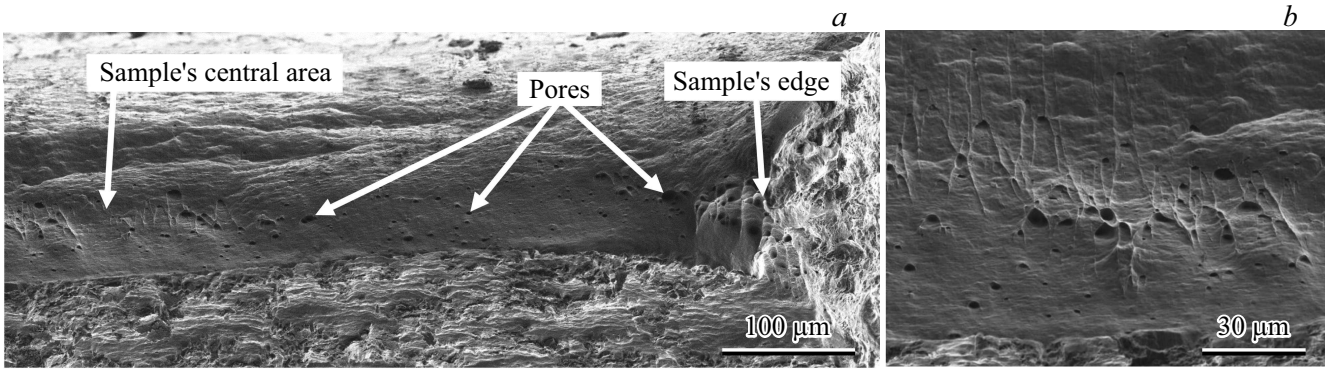

Figure 1. *a* — fracture structure of AD1 grade aluminum samples after creep test. *b* — enlarged images of the central area of the destroyed sample, demonstrating a dimpled character (cup-like depressions containing micropores). Scanning electron microscopy.

electron microscopy). Thin films for TEM were produced by the focused ion beam method on a FEI Scios scanning electron microscope, with the possibility of analyzing backscattered diffraction at an accelerating voltage of 20 kV and the orientation of the sample surface by 70° to the direction of the electron beam. The TSL OIM Data Collection and TSL OIM Analysis programs, respectively, were used to build disorientation and data processing histograms, version 6.21 firms EDAX.

The volume of damage caused by creep was estimated by a precision density measurement method with relative accuracy $\Delta\rho/\rho$ 0.01% on Shimadzu 120D analytical scales using the SMK-301 additional equipment. This method allows us to determine the density with high accuracy necessary to assess changes in the density of samples after various impacts [5]. Information about the presence and parameters of nanopores was obtained by the method of small-angle X-ray scattering, which was used in previous works on the identification of the nanoporosity arising from IPD [4,5].

3. Results and discussion

Structural studies of microcrystalline aluminum samples tested in the creep mode were carried out mainly on and near the fracture surface (fracture). The study of the evolution of the structure during the creep of polycrystalline metals (including aluminum) for the entire working part of the samples was carried out by the authors earlier [14,15].

Ley us consider the experimental data. On the surface of the samples near the site of destruction (Fig. 1), the presence of pores of the order of $1-5\,\mu$m is noted (marked with arrows). According to fractographic analysis, the structure of the central area of the fracture surface of the samples after creep tests has a form characteristic of viscous fracture (Fig. 1, *a* and *b*), as evidenced by the cup (well) structure of the fracture. The wells contain pores having a predominantly equiaxed shape along the edges of the destroyed sample and elongated in the central part of the fracture of the sample. In the central part of the fracture surface there are areas of viscous cleavage with traces of plastic deformation. The destruction of the sample occurs with the formation and fusion of pores of the order of $1-10\,\mu$m.

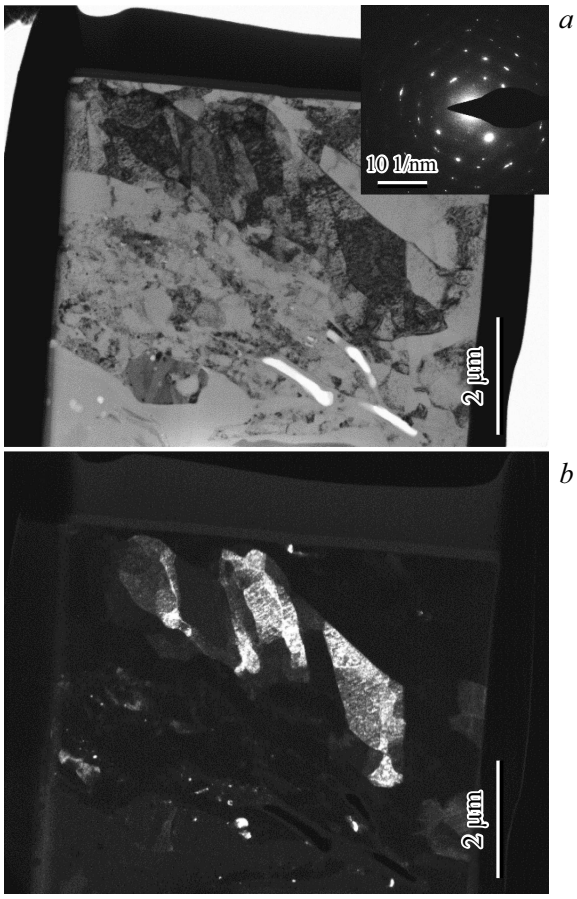

Figure 2. Microstructure of the aluminum alloy sample AD1 after the creep test (fracture region): *a* — light-field, *b* — dark-field image obtained in the reflex (200) marked on the microdifraction. TEM.

Chemical composition of aluminum grade AD1 according to GOST 4784-97

Alloy AD1	Element content, wt%, Al — basis							
	Fe	Si	Ti	Zn	Cu	Mg	Mn	Impurities
Req.	≥ 0.3	≥ 0.3	≥ 0.15	≥ 0.1	≥ 0.05	≥ 0.05	≥ 0.025	≥ 0.05

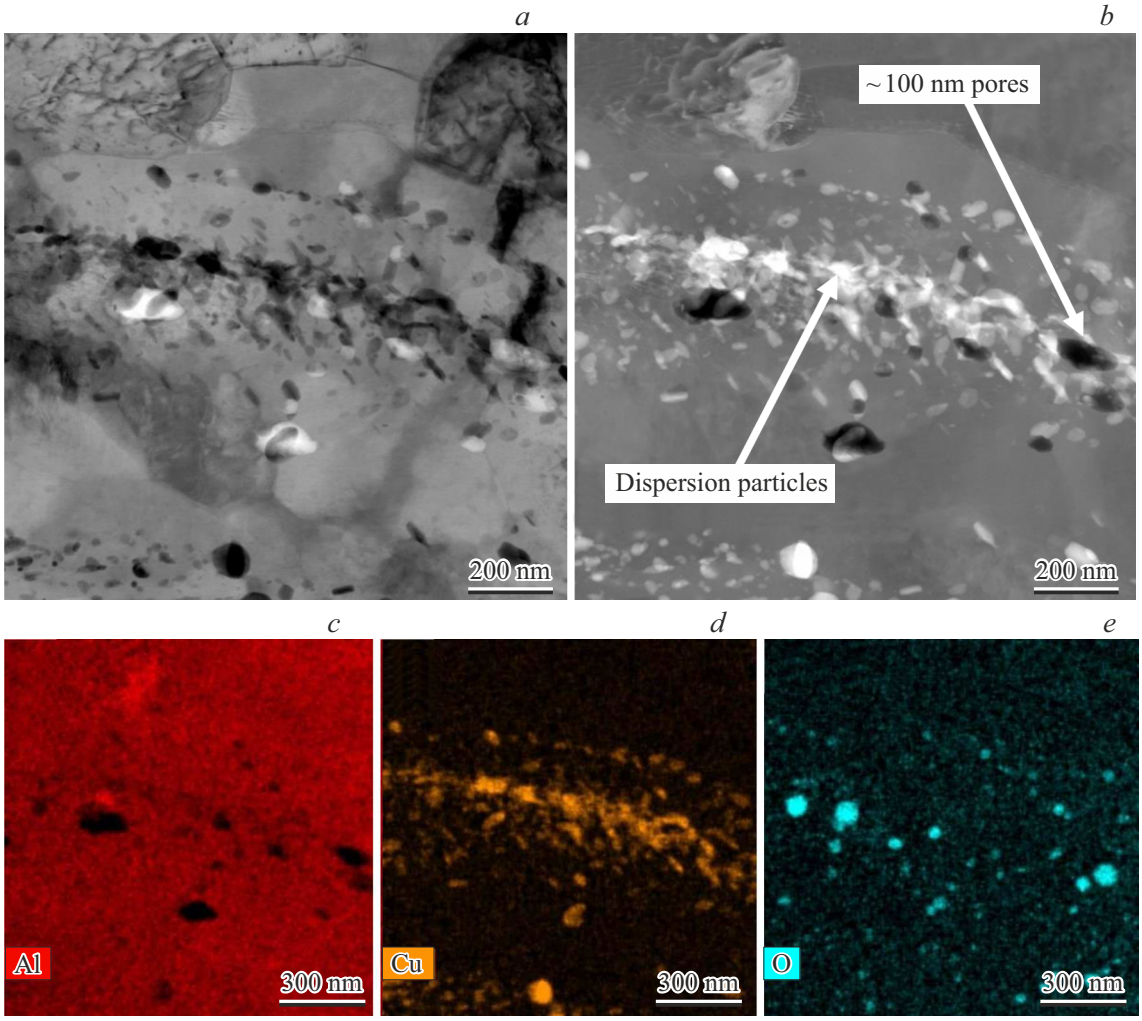

Figure 3. Images of the microstructure in the fracture region of the sample of the alloy under study after the creep test: *a* — light-field image; *b* — dark-field image in PREM; *c*–*e* — maps of the distribution of elements.

Fig. 2 shows images of the microstructure of a sample that was cut from an area near the site of destruction. The dark-field image shows that subgrains with disorientation boundaries are formed inside the grains during creep (this is evidenced by the azimuthal nature of the distribution of reflexes on microdifraction, insert in Fig. 2, *a*). The elements of the grain-subgrain structure have a size of the order of 0.5μm. Internal cavities of an elongated shape are observed with a length of the order of $2\,\mu$m and a width of $0.3\,\mu$m.

In the images obtained at high magnifications, fine particles with formed nanoscale pores with a diameter of about 100 nm are observed (Fig. 3). According to energy-dispersive X-ray spectroscopy, the dispersed particles are aluminum and copper oxides, which is confirmed by the distribution maps of the elements shown in Fig. 3, *c*–*e*.

As already noted, a small part of the research was carried out in the working part of the sample away from the destruction zone. Electron microscopic images of the sample structure away from the fracture area are shown in Fig. 4. On the dark-field images obtained in various reflexes of the microdifraction pattern, a contrast from grains of the order of $2\,\mu$m is observed.

Maps of the grain structure in both studied areas of the sample (Fig. 5), as well as histograms of grain size distribution (Fig. 6) were built. There is a noticeable decrease in the average grain size in the fracture region in

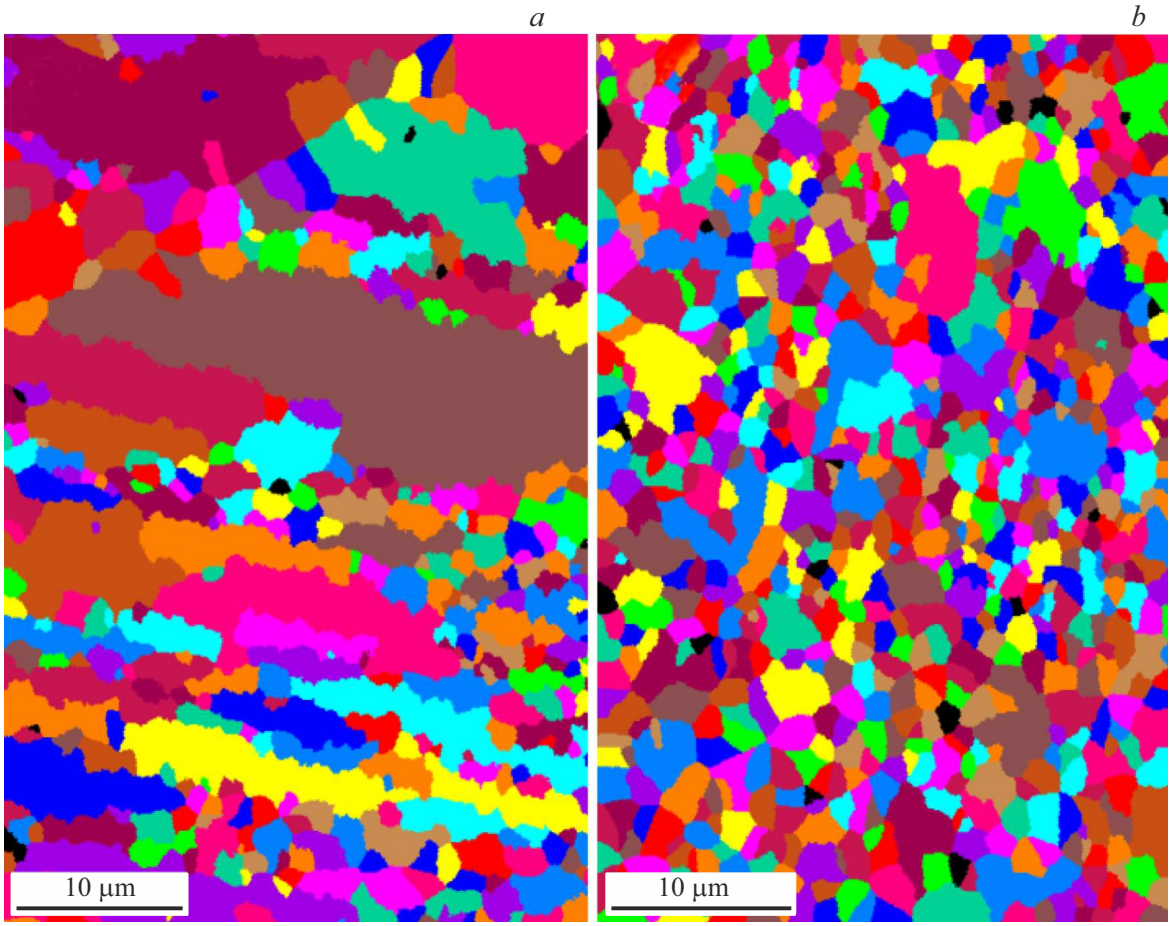

Figure 4. Microstructure of the AD1 aluminum sample after the creep test, which was manufactured away from the fracture area: *a* — light-field image; *b* — dark-field image obtained in a reflex from the plane $(-11-1)$ microdifraction. TEM.

comparison with the area of the working base of the sample. The shape of the structure elements also changes from predominantly elongated (formed by rolling) to equiaxed.

The histogram of grain size distribution obtained from the area away from the destruction site (Fig. 6, *a*) shows the formation of large grains larger than $5\,\mu$m in the creep process, and there are no such grains in the destruction area (Fig. 6, *b*). In the fracture region, the average grain size is $1.6 \pm 0.2\,\mu$m, and away from it — of the order of $2 \pm 0.3\,\mu$m. When constructing maps by Electron backscatter diffraction (EBSD) in a scanning electron microscope of misorientation and dimensions of structural elements, small-angle boundaries are not taken into account, whereas according to TEM data, a sufficiently large number of them were observed, and the size of the subgrains measured in this case was on the order of $0.5\,\mu$m. Thus, taking into account this feature, the average size of the elements of a grain-subgrain mixture of recrystallized in the fracture region is of the order of $\geq 1\,\mu$m.

Histograms of grain distribution by the angle of disorientation are constructed (Fig. 7). The proportion of high-angle grain boundaries (HAGB) in the fracture region is noticeably higher (about 70%) the working base of the sample (about 50%).

Thus, the analysis of histograms showed that the average grain size $(1.6-2.0\,\mu$m) near and far from the rupture site is almost the same and coincides with the grain size in the initial (pre-test) samples $(1.5\,\mu$m). It has also been established that pores of structural size are formed near and far from the rupture site $(1-2\,\mu$m) and their larger conglomerates $(\geq 5\,\mu$m).

The data on pores are in good agreement with the results obtained by the authors earlier in the study of creep in the region of moderate temperatures of coarser-grained crystalline aluminum [13,14]. But in [13,14], the formation of a set of pores and cracks with a size of $\sim 0.1\,\mu$m was first established during creep, the accumulation rate and concentration of which in thin near-surface layers are $1-3$ orders of magnitude greater than in the volume of samples[1] [13]. That is why a large (up to 1%) decompression accumulates in the near-surface layers, forming a fracture.

[1] The intensification of micro-destruction in the near-surface layer is justified by the peculiarities (in comparison with the volume) of its dislocation and disclosure structure [13,14].

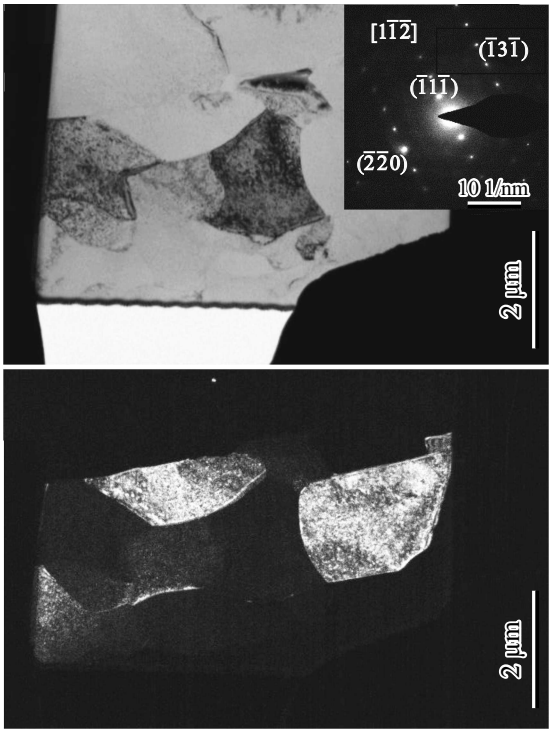

Figure 5. Microstructure of the alloy under study after the creep test: *a* — away from the fracture zone; *b* — fracture zone. Diffraction of backscattered electrons in SEM.

In the theoretical works [17,18], the physical mechanism of the formation of pore-like cracks of the size $\sim 0.1\,\mu$m is substantiated and an estimate of the density defect ($\sim 1\%$) caused by micro-gaps and preceding macro-destruction is given. Thus, experimental and theoretical data indicate a special role of surface layers under prolonged loading. Taking into account these data, for microcrystalline aluminum tested in the creep mode by the SAXS method and the density measurement method, an assessment of the damaged surface layer with a thickness of $\sim 5\,\mu$m near the fracture site (chip) was carried out. The SAXS method revealed the presence of pores in this layer with a size of $\sim 0.12\,\mu$m and a concentration of $\sim 10^{12}\,\mathrm{m}^{-2}$; the volume of density defect ($\Delta\rho/\rho$) from these the portion was 1.6%. The density defect according to the relative density reduction data in the same layer is quite close in order of magnitude, but slightly exceeds the SAXS data (1%). This is obviously due to the fact that the SAXS method captures only pores with a size of $\leq 0.3\,\mu$m, and the density measurement method also takes into account larger coagulations of these nanopores. The close values of decompression obtained by two independent methods confirm the reliability of information about the level of damage to the surface layer near the fracture site of microcrystalline aluminum.

Interesting new data were obtained by analyzing the fracture surface of an aluminum sample. Firstly, a grain structure of the size $\sim 0.5\,\mu$m is formed only on the rupture surface, which is 3–10 times smaller than in other areas of the sample. Secondly, the proportion high-angle grain boundaries (HAGB) on the rupture surface is noticeably greater ($\geq 20\%$) than that of grain boundaries outside the rupture surface. Thirdly, it is on the rupture surface (near impurity inclusions) that nanoscale pores are observed; however, it seems that inclusions in this case are only an additional factor stimulating the formation of nanopores on the rupture surface. Indeed, earlier the authors found the formation of nanopores on the surface of the rupture of cold-rolled to large degrees of thickness $1-2\,\mu$m silver, in which there were no impurities (Fig. 8) [14].

All three of these features of the microstructure of the fracture surface of microcrystalline aluminum are characteristic of the microstructure of metals and alloys obtained by the method of intensive plastic deformation. This allows us to assume that such a deformation is realized in the fracture zone (at the fracture).

In conclusion, we will analyze the nature of the influence of impurities on the formation of pores and some data on the effect of impurity inclusions and associated porosity on long-term strength. It is known [19], that impurities segregating on the inner surfaces of the interface can also contribute to pore formation and pore growth at grain

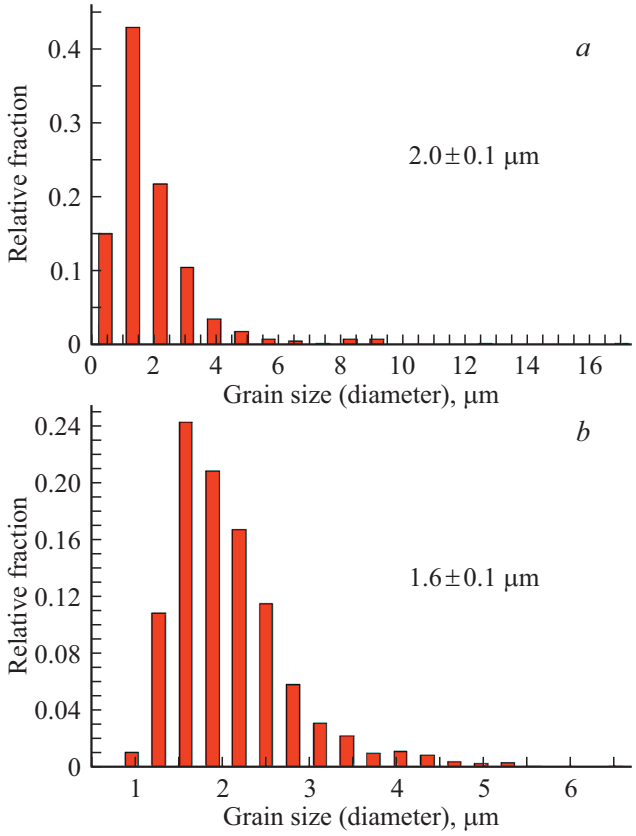

Figure 6. Histogram of grain size distribution in samples of crystallized aluminum grade AD1 after the creep test: *a* — away from the fracture area; *b* — near the fracture surface. The data were obtained by backscattered electron diffraction in SEM.

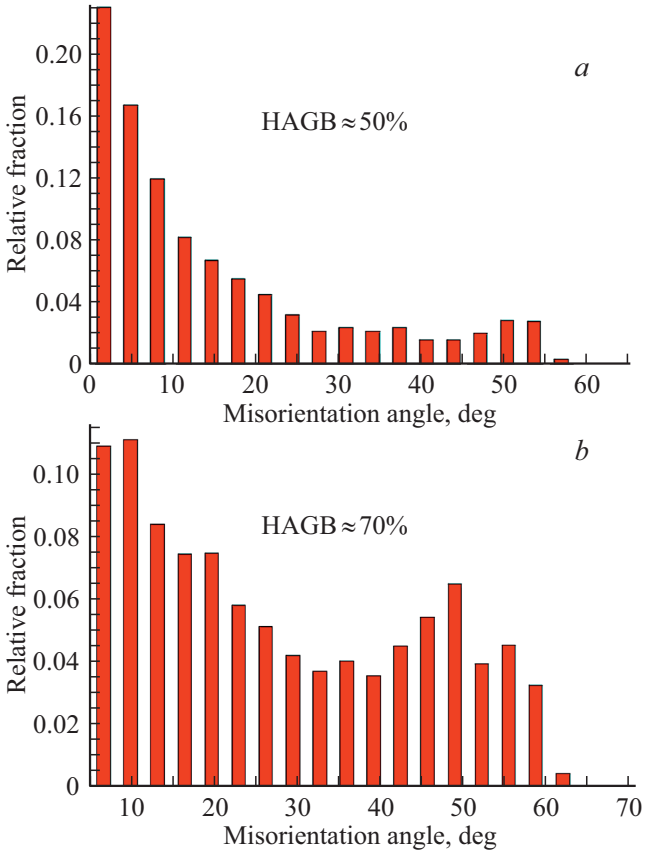

Figure 7. Histograms of the distribution of grain boundaries by the angle of disorientation in samples of crystallized aluminum grade AD1 after the creep test: *a* — away from the fracture zone; *b* — fracture zone. The data were obtained by backscattered electron diffraction in SEM.

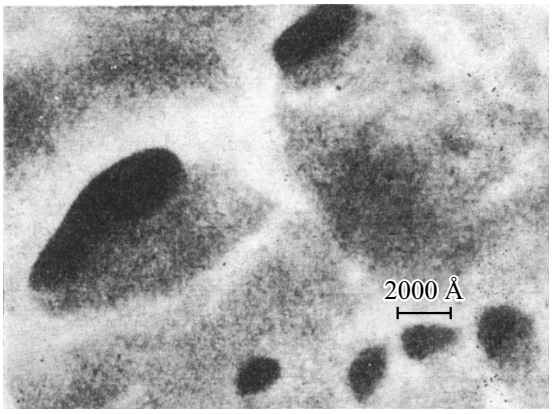

Figure 8. Discontinuities on the Ag discontinuity surface (data [14]).

boundaries and particles of dispersed phases. Usually, this effect is associated with a decrease in the mobility of grain boundaries by impurities, manifestations of the effect of increasing their diffusion permeability of the boundaries and reducing surface energy during segregation of horophilic impurities. In the work [17] cited above, the position is substantiated that the formation of cracks on particles is preceded by the formation of pores of critical size on them $r_c = 2\gamma_m/\sigma_n$, where γ_m — specific surface energy of the matrix; σ_n — normal stress on the particle. For this reason, the presence of elastic stresses and reducing the surface energy of horophilic impurities significantly facilitate the nucleation of pores, regardless of the place where it occurs.

Impurities and pores formed (especially during prolonged loading) near them affect the long-term strength of metals and alloys. It has been established that impurity inclusions leading to a more intense formation of nanoporosity during IPD significantly affect the stability and mechanical properties of metallic SMG materials [5]. When tested in creep and fatigue mode at moderate temperatures, such nanoporosity leads to a decrease in the durability (and resource) of high-strength SMG metals and alloys. When tested in the field of high-temperature creep, impurity inclusions, due to their stabilizing effect on the evolution of grain boundaries, can neutralize the negative role of nanoporosity.

4. Conclusion

Analysis of the histogram showed that the average grain size tested in the creep mode of microcrystalline aluminum far and near the place of its rupture, as well as in the initial (before the test) state, is almost the same. But the formation of a subgrain structure with an average size of $0.5\,\mu$m is also observed in the gap zone.

It is established that in the central part of the rupture surface (fracture), a well with traces of plastic deformation and pores, characteristic of viscous fracture, is formed.

It has been found that in thin near-surface layers, many submicropores appear at the site of rupture, the density defect (damage) from which and their merged formations is about 1%.

The size of the subgrain structure on the surface of the gap is 3–10 times smaller, and the proportion of high-angle grain boundaries (HAGB) is $\sim 25\%$ larger than that of grains near and away from the gap site. In addition, nanoscale pores were found on the surface of destruction. These three structural features are characteristic of metals obtained by the IPD method. This allows us to assume the identity of the nature of the processes occurring in the destruction zone and in the case of IPD.

The relationship between impurity inclusions and nanoporosity formed during plastic deformation (including IPD), as well as the role of inclusions and nanopores for the long-term strength (and resource) of microcrystalline and SMG metals and alloys is analyzed.

Funding

The authors acknowledge that the financial support for this study was provided by the Russian Foundation for Basic Research (project No. 19-58-26005) and the Czech

Science Foundation (project No. 20-14450J). Structural studies were carried out using scientific equipment of the Central Research Center of the Federal Research Institute „Crystallography and Photonics“ RAS (Moscow).

Conflict of interest

The authors declare that they have no conflict of interest.

References

[1] V.R. Regel, A.I. Slutsker, E.E. Tomashevsky. Kineticheskaya priroda prochnosti. Nauka, M. (1974). 536 p. (in Russian).
[2] Yu.I. Rabotnov. Polzuchest' elementov konstruktsii. Nauka, M. (1996). 752 p. (in Russian).
[3] L.M. Kachanov. Osnovy mekhaniki razrusheniya. Nauka, M. (1974). 312 p. (in Russian).
[4] V.I. Betekhtin, A.G. Kadomtsev, V. Sklenicka, I. Saxl. FTT **49**, *10*, 1787 (2007).
[5] V.I. Betekhtin, A.G. Kadomtsev, M.V. Narykova. FTT **62**, *2*, 267 (2020). (in Russian).
[6] R. Lapovok, D. Tomus, J. Mang, Y. Estin, T.C. Lowe. Acta Mater. **57**, *10*, 2909 (2009).
[7] J. Ribbe, G. Schmitz, D. Gundarev, Y. Estin, Y. Amouyal, S.V. Divinski. Acta Mater. **61**, *14*, 5477 (2013).
[8] S.V. Divinski, G. Reglitz, I.S. Golovin, M. Peterlechner, R. Lapovok, Y. Estin, G. Wilde. Acta Mater. **82**, 11 (2015).
[9] V.N. Perevezentsev, A.S. Pupynin, A.E. Ogorodnikov. ZhTF **88**, *10*, 1539 (2018). (in Russian).
[10] J. Čižek, M. Janeček, O. Sbra, R. Kužel, Z. Barnovská, I. Procházka, S.V. Dobatkin. Acta Mater. **59**, *6*, 2322 (2011).
[11] V.V. Mishakin, V.N. Perevezentsev, M.Yu. Scherban, V.A. Klyushnikov, T.A. Gracheva, T.A. Kuzmicheva. Defektoskopiya **6**, 57 (2015) (in Russian).
[12] S.V. Divinski, G. Reglitz, H. Rosner, Y. Estrin, G. Wilde. Acta Mater. **59**, *5*, 1974 (2011).
[13] B.I. Betekhtin, A.G. Kadomtsev. FTT **47**, *5*, 801 (2005). (in Russian).
[14] V.I. Betekhtin, V.I. Vladimirov, A.G. Kadomtsev, A.I. Petrov. Problemy prochnosti **7**, 38 (1979). (in Russian)
[15] P.G. Cheremskoy, V.V. Slezov, V.I. Betekhtin. Pory v tviordom tele. Energoatomizdat, M., (1990). 376 p. (in Russian).
[16] Y.R. Kolobov. Russ. Phys. J. **61**, *4*, 611 (2018).
[17] V.I. Vladimirov. Fizicheskaya priroda razrusheniya metallov. Metallurgiya, M. (1984). 280 s. (in Russian).
[18] V.I. Vladimirov, A.E. Romanov. Disklinatsii v kristallakh. Nauka, L. (1986). 224 p. (in Russian).
[19] Y.R. Kolobov. Diffuzionno-kontroliruemye protsessy na granitsakh zeren i plastichnost' metallicheskikh polikristallov (Diffusion-controlled processes at grain boundaries and plasticity of metallic polycrystals). Nauka, Novosibirsk (1998). 184 p. (in Russian).